Experimental Evidence of a Phase Transition in a Closed Turbulent Flow

P.-P. Cortet, Arnaud Chiffaudel, François Daviaud, Bérengère Dubrulle

Experimental Evidence of a Phase Transition in a Closed Turbulent Flow

P.-P. Cortet, A. Chiffaudel, F. Daviaud, and B. Dubrulle

CEA, IRAMIS, SPEC, CNRS URA 2464, Groupe Instabilités et Turbulence, 91191 Gif-sur-Yvette, France

(Received 3 May 2010; published 19 November 2010)

We experimentally study the susceptibility to symmetry breaking of a closed turbulent von Kármán swirling flow from Re = 150 to Re $\simeq 10^6$. We report a divergence of this susceptibility at an intermediate Reynolds number Re = $\mathrm{Re}_\chi \simeq 90\,000$ which gives experimental evidence that such a highly space and time fluctuating system can undergo a "phase transition." This transition is furthermore associated with a peak in the amplitude of fluctuations of the instantaneous flow symmetry corresponding to intermittencies between spontaneously symmetry breaking metastable states.

DOI: 10.1103/PhysRevLett.105.214501 PACS numbers: 47.20.Ky, 47.27.Cn

Phase transitions are ubiquitous in physical systems and are generally associated with symmetry breaking. For example, ferromagnetic systems are well known to undergo a phase transition from paramagnetism to ferromagnetism at the Curie temperature T_c. This transition is associated with a symmetry breaking from the disordered paramagnetic—associated with a zero magnetization—toward the ordered ferromagnetic phase—associated with a finite magnetization [1]. In the vicinity of T_c, a singular behavior characterized by critical exponents is observed, e.g., for the magnetic susceptibility to an external field. In the context of fluid dynamics, symmetry breaking also governs the transition to turbulence, that usually proceeds, as the Reynolds number Re increases, through a sequence of bifurcations breaking successively the various symmetries allowed by the Navier-Stokes equations coupled to the boundary conditions [2]. Finally, at large Reynolds number, when the fully developed turbulent regime is reached, it is commonly admitted that all the broken symmetries are restored in a statistical sense, the statistical properties of the flow not depending anymore on Re [3]. However, recent experimental studies of turbulent flows have disturbed this vision raising intriguing features such as finite lifetime turbulence [4]—questioning the stability of the turbulent regime—and the possible existence of turbulent transitions [5–11]. Consequently, despite the fact that turbulent flows are intrinsically out-of-equilibrium systems, one may wonder whether the observed transitions can be interpreted in terms of phase transitions with a symmetry-breaking or susceptibility divergence signature. In this Letter, we introduce a susceptibility to symmetry breaking in a von Kármán turbulent flow and investigate its evolution as Re increases from 150 to 10^6 using stereoscopic particle image velocimetry (PIV). We observe a divergence of susceptibility at a critical Reynolds number Re = $\mathrm{Re}_\chi \simeq 90\,000$, which sets the threshold for a possible turbulent "phase transition." Moreover, this divergence is associated with a peak in the amplitude of the fluctuations of the flow instantaneous symmetry.

Our experimental setup consists of a Plexiglas cylinder of radius $R = 100$ mm filled up with either water or water-glycerol mixtures. The fluid is mechanically stirred by a pair of coaxial impellers rotating in opposite directions (Fig. 1). The impellers are flat disks of radius $0.925R$, fitted with 16 radial blades of height $0.2R$ and curvature radius $0.4625R$. The disks' inner surfaces are $1.8R$ apart setting the axial distance between impellers from blades to blades to $1.4R$. The impellers rotate, with the convex face of the blades pushing the fluid forward, driven by two independent brushless 1.8 kW motors. The rotation frequencies f_1 and f_2 can be varied independently from 1 to 12 Hz. Velocity measurements are performed with a stereoscopic PIV system provided by DANTEC Dynamics. The data provide the radial u_r, axial u_z, and azimuthal u_φ velocity components in a meridian plane on a 95×66 points grid with 2.08 mm spatial resolution through time series of 400 to 27 000 fields regularly sampled, at frequencies from 1 to 15 Hz, depending on the turbulence intensity and the related need for statistics. The control parameters of the

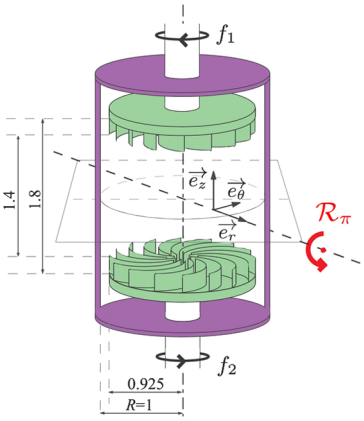

FIG. 1 (color online). Schematic view of the experimental setup and the impellers' blade profile. The arrow on the shaft indicates the impeller rotation direction studied. Symmetry: The system is symmetric regarding any $\mathcal{R}_\pi$ rotation of angle π around any line of the equatorial plane which crosses the rotation axis.

studied von Kármán flow are the Reynolds number $\mathrm{Re} = \pi(f_1 + f_2)R^2/\nu$, where ν is the fluid viscosity, which controls the intensity of turbulence and the rotation number $\theta = (f_1 - f_2)/(f_1 + f_2)$, which controls the asymmetry of the forcing conditions. The rotation frequencies $f_{1,2}$ are regulated by servo loop control and we obtain for θ a typical absolute precision of 1×10^{-3} and time fluctuations of the order of $\pm 2 \times 10^{-4}$. The correlation between these fluctuations and the flow dynamics is negligible.

When $\theta = 0$, the experimental system is symmetric with respect to any $\mathcal{R}_\pi$ rotation exchanging the two impellers: the problem conditions are invariant under π rotation around any radial axis passing through the center of the cylinder (Fig. 1). The symmetry group for such experimental systems is $O(2)$ [12]. When $\theta \neq 0$, the experimental system is no longer $\mathcal{R}_\pi$ symmetric, and the symmetry switches to the $SO(2)$ group of rotations. However, the parameter θ, when small but nonzero, can be considered as a measure of the distance to the exact $O(2)$ symmetry: the $SO(2)$ system at small θ can be considered as a slightly broken $O(2)$ system [13,14]. Depending on the value of θ, the flow can respond by displaying different symmetries: (i) the exact $\mathcal{R}_\pi$-symmetric flow composed of two toric recirculation cells separated by an azimuthal shear layer located at $z = 0$ when $\theta = 0$ [Figs. 2(a) and 2(c)]; (ii) an asymmetric two-cells flow, the shear layer being closer to the slowest impeller ($z \neq 0$), when $\theta \neq 0$ [Figs. 2(b) and 2(d)]; (iii) and finally, a fully nonsymmetric one-cell flow, the whole shear layer being concentrated in between the blades of the slowest impeller, when θ becomes large enough [7,10,15].

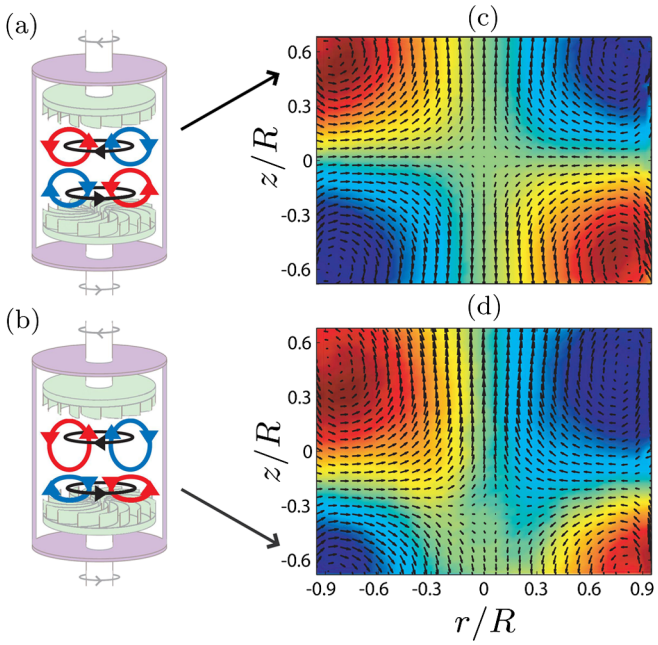

FIG. 2 (color online). (a),(b) Schematic drawings of the flow topology and (c),(d) corresponding experimental maps of mean velocity field of the turbulent von Kármán flow at $\mathrm{Re} = 800\,000$ for (c) $\theta = 0$ ($\bar{I} = 0$) and (d) $\theta = -0.0147$ ($\bar{I} < 0$). The color maps the azimuthal velocity u_φ, from blue to red ("jet" color map), whereas the arrows map the (u_r, u_z) field. The resolution has been reduced by a factor of 2 for better visibility. The $r \leftrightarrow -r$ symmetry in (c) and (d) reveals that the time-averaged mean fields are axisymmetric.

In order to quantify the distance of the flow to the $\mathcal{R}_\pi$ symmetry, we use the normalized and space-averaged angular momentum $I(\mathrm{Re}, \theta, t)$ as order parameter:

$$I(t) = \frac{1}{\mathcal{V}} \int_{\mathcal{V}} r dr d\varphi dz \frac{r u_\varphi(t)}{\pi R^2 (f_1 + f_2)},$$

where $\mathcal{V}$ is the volume of the flow [16]. An example of time variation of $I(t)$ at $\theta = 0$ in the turbulent regime is provided in Fig. 3. We assume that ergodicity holds, meaning that the instantaneous turbulent flow is exploring in time its energy landscape according to its statistical probability. In this framework, the time-average value $\bar{I}$ of $I(t)$ is equivalent to a statistical mechanics ensemble average providing the average is performed over a long enough duration in order to correctly sample the slowest time scales. Then, using this ensemble averaged order parameter, we define a susceptibility of the flow to symmetry breaking as $\chi_I = \partial \bar{I}/\partial\theta|_{\theta=0}$. Note that $\bar{I}$ is proportional to the mean altitude z_s of the shear layer which is the natural measure of the flow symmetry. Contrary to z_s, $I(t)$ is defined for any instantaneous velocity field, including turbulent ones.

In the nonfluctuating laminar case, when $\theta = 0$, $\bar{I} = 0$ due to the symmetry of the flow. In contrast, as θ drifts away from 0, the value of the angular momentum $\bar{I}$ becomes more and more remote from zero as the asymmetry of the flow grows. In such a framework, there is a formal analogy between ferromagnetic and turbulent systems. For ferromagnetism [respectively, turbulence], the order parameter is the magnetization $M(T, h)$ [the angular momentum $I(\mathrm{Re}, \theta)$], the symmetry-breaking parameter is the external applied field h [the relative driving asymmetry θ], the control parameter is the temperature T [the Reynolds number Re, or a function of it].

In the following, we first investigate the influence of turbulence on $\bar{I}$ and χ_I as Re increases from 150 to 10^6. In the laminar flow at $\mathrm{Re} = 150$, the symmetry parameter $\bar{I} = I(t)$ evolves linearly with θ [Fig. 4(c)] and the susceptibility is $\chi_I = 0.240 \pm 0.005$. Increasing the Reynolds number, one expects to reach fully developed turbulence around $\mathrm{Re} = 10\,000$ [10]. In such turbulent regimes, velocity fields

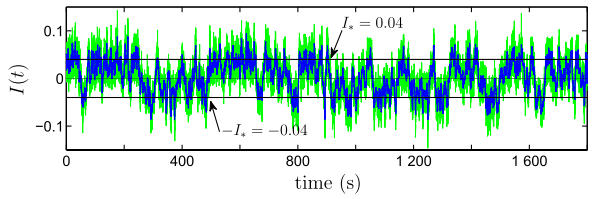

FIG. 3 (color online). Global angular momentum $I(t)$ as a function of time for an experiment performed at $\mathrm{Re} = 43\,000$ for $\theta = 0$. Green (light gray) dots are PIV data sampled at 15 Hz, and blue (dark gray) dots correspond to 1 Hz low-pass filtered data $I_f(t)$. Eye-guiding lines have been drawn at $I(t) = \pm I_* = \pm 0.04$.

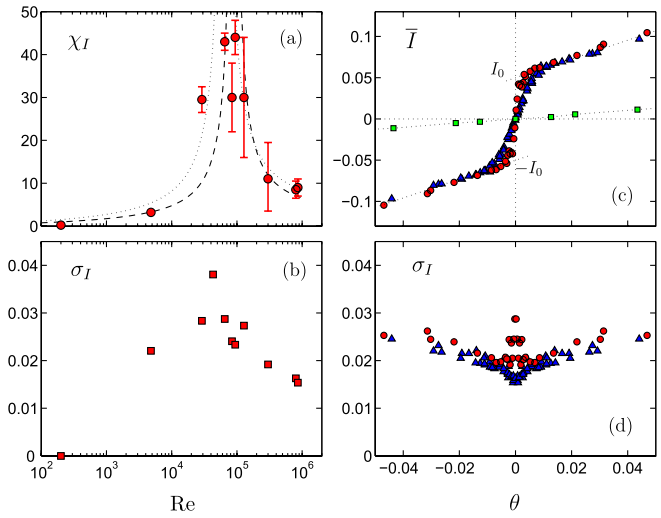

FIG. 4 (color online). Reynolds number dependence of (a) susceptibility to symmetry breaking χ_I of the von Kármán mean flow at $\theta = 0$ and (b) standard deviation σ_I of the global angular momentum $I(t)$ at $\theta = 0$. In (a), the dotted line corresponds to the mean field theory approach with a critical Reynolds number $\mathrm{Re}_\chi = 70\,000$ and the dashed line to $\mathrm{Re}_\chi = 90\,000$. (c) Global angular momentum $\bar{I}$ and (d) standard deviation σ_I as a function of θ for $\mathrm{Re} = 150$ (green □), $\mathrm{Re} = 65\,000$ (red ○), and $\mathrm{Re} = 800\,000$ (blue △). In (a) and (b), horizontal error bars are of the order of the marker size. In (a) vertical error bars are computed as the maximum error that can arise from the sharp dependence of σ_I with θ around $\theta = 0$.

of von Kármán flows are characterized by a high level of intrinsic fluctuations, i.e., fluctuations of the same order of magnitude as the mean values [15]. Therefore, even when $\theta = 0$, the $\mathcal{R}_\pi$ symmetry is of course broken for the instantaneous flow. However, as is usually observed for classical turbulence, this symmetry is restored for the time-averaged flow [Fig. 2(c)], which proves that time averages are long enough to correctly sample the slowest flow time scales. Then, as in the case of the laminar flow, when θ is varied, we observe the breaking of the $\mathcal{R}_\pi$ symmetry of the mean flow [Fig. 2(d)].

In Fig. 4(c), we see that, at $\mathrm{Re} = 800\,000$, in the close vicinity of $\theta = 0$, $\bar{I}(\theta)$ evolves actually much more rapidly with θ than in the laminar case with the susceptibility being larger by more than 1 order of magnitude: $\chi_I = 9 \pm 1$. Therefore, turbulence seems to enhance dramatically the sensitivity of the flow to symmetry breaking. Furthermore, for intermediate $\mathrm{Re} = 65\,000$, the slope of $\bar{I}(\theta)$ around $\theta = 0$ is even much steeper—$\chi_I = 43 \pm 1$—than for $\mathrm{Re} = 800\,000$. In Fig. 4(a), we plot the susceptibility with respect to Re. We see that the susceptibility actually grows by more than 2 orders of magnitude—from 0.24 to 46—between $\mathrm{Re} = 150$ and $\mathrm{Re} \simeq 90\,000$, before decreasing by a factor of 4 between $\mathrm{Re} \simeq 90\,000$ and $\mathrm{Re} = 800\,000$. These results suggest a critical behavior for $\chi_I(\mathrm{Re})$ near $\mathrm{Re} = \mathrm{Re}_\chi = 90\,000 \pm 10\,000$: a divergence—revealing a continuous second order phase transition—or only a maximum—revealing either a subcritical bifurcation or a continuous transition with finite-size effect. This cannot be experimentally tested further since the highest measured χ_I are already of the order of the highest measurable value considering the θ precision of our setup. For higher $|\theta|$, we observe a crossover—for the slope—in the curve $\bar{I}(\theta)$ at $|\theta_r| = (6 \pm 1) \times 10^{-3}$ for $\mathrm{Re} = 800\,000$ and very close to $\theta = 0$, at $|\theta_r| = (0.9 \pm 0.15) \times 10^{-3}$, for $\mathrm{Re} = 65\,000$ [Fig. 4(c)]. For $|\theta| > |\theta_r|$, we recover the laminar slow evolution of $\bar{I}$ with θ up to $\theta = \pm 0.1$ where the flow bifurcates to the one-cell topology (not shown). Since $\bar{I}(\theta)$ is quite independent of Re for $|\theta| > |\theta_r|$ at large Re, we can extrapolate this linear behavior to $\theta = 0$. This extrapolation describes the ideal behavior at critical Reynolds number Re_χ if χ_I diverges: a jump of $\bar{I}$ between $-I_0$ and $+I_0$, where $I_0 \simeq 0.05$. This can be interpreted as a spontaneous "turbulent momentization" I_0 at $\theta = 0$—possibly affected by finite-size effects—by analogy with the spontaneous magnetization M_0 at zero external field for ferromagnetism. It is also similar to the experimental results of [17].

A signature of this momentization can be seen on the instantaneous global angular momentum $I(t)$ for Re near the peak of susceptibility and $\theta = 0$ (e.g., in Fig. 3). Indeed, one observes that $I(t)$ does not remain near zero (its mean value) but shows a tendency to lock preferentially on the plateaus $\pm I_*$ with $I_* = 0.04 \simeq I_0$. Therefore, the turbulent flow explores a continuum of metastable symmetry-breaking patterns evidenced by $-0.04 \lesssim I_f(t) \lesssim 0.04$, $I_f(t)$ being the 1 Hz low-pass filtered value of $I(t)$. The global angular momentum actually fluctuates very much along time with two separate time scales: fast fluctuations related to "traditional" small scale turbulence and time intermittencies corresponding to residence time of few tens of seconds. If one performs a time average over one of these intermittent periods only, one obtains a time localized "mean" flow, which breaks spontaneously the symmetry, analogous to what is obtained for true mean flows when $\theta \neq 0$, as presented in Figs. 2(b) and 2(d).

The presence of strong fluctuations is not surprising here: close to a phase transition we expect critical fluctuations. To check this, we compute the standard deviation $\sigma_I(\mathrm{Re}, \theta)$. Figure 4(b) shows, for $\theta = 0$, how σ_I varies from zero in the laminar case to finite values for highly turbulent flows going through a maximum at Reynolds number $\mathrm{Re} = \mathrm{Re}_\sigma = 45\,000 \pm 10\,000$ located below the peak of susceptibility at Re_χ. Additionally, in Fig. 4(d), the dependence of σ_I as a function of the symmetry control parameter θ reveals a strong difference between the two Reynolds numbers shown: $\sigma_I(\theta)$ presents a sharp and narrow peak at $\theta = 0$ for $\mathrm{Re} = 65\,000$, which does not exist for $\mathrm{Re} = 800\,000$. The amplitude of this peak from its bottom to its top actually measures the additional amount of low frequency symmetry fluctuations due to the multistability. This amount of fluctuations appears to be connected to the susceptibility increase below Re_χ.

The previous experimental results set a strong connection between the spontaneous symmetry fluctuations of the flow

and the mean flow response to the system symmetry breaking: the interpretation of the large fluctuations of $I(t)$ in terms of multistability suggests that the strong observed linear response of the mean flow [Fig. 4(c)] with respect to θ in the close vicinity of $\theta = 0$ is the result of a temporal mixing between the metastable states in different proportions.

Nevertheless, as the Reynolds number is varied, two distinct maxima have been evidenced in our turbulent flow: one for the susceptibility χ_I to the $O(2)$ symmetry breaking near $\mathrm{Re} = \mathrm{Re}_\chi \simeq 90\,000$, and the other for the standard deviation of the global angular momentum $I(t)$ near $\mathrm{Re} = \mathrm{Re}_\sigma \simeq 45\,000$. In this Reynolds number range, the turbulence is generally expected to be fully developed; i.e., any nondimensional characteristic quantity of the flow should be Re independent. This is definitively not the case in this von Kármán experiment. Actually, visual observations of the flow reveal an increase of the average azimuthal number m of large scale vortices in the shear layer from $m = 3$ to $m = 4$ through an Eckhaus-type transition, between Re_σ and Re_χ. In the following, we make the hypothesis that at least one critical phenomenon exists in the range $50\,000 \lesssim \mathrm{Re} \lesssim 100\,000$. Using the turbulent von Kármán-ferromagnetism analogy, we can check how classical mean field predictions for second order phase transition apply to our system. In terms of susceptibilities, it predicts a critical divergence at a temperature T_c: $\chi \propto |T - T_c|^{-1}$. Since the logarithm of the Reynolds number has already been proposed as the control parameter governing the statistical temperature of turbulent flows—$T \sim 1/\log\mathrm{Re}$ [18]— this prediction translates in our case into $\chi_I \propto |1/\log\mathrm{Re} - 1/\log\mathrm{Re}_c|^{-1}$. This formula reasonably describes our data with Re_c between typically 70 000 and 90 000 [Fig. 4(a)] supporting the asymmetry between the two branches even with a unique exponent -1. As far as fluctuations are concerned, it is difficult to find a reasonable critical exponent for σ_I. However, the results show that the maxima for χ_I and σ_I are clearly separated. This is at variance with classical phase transition theory, stating, e.g., in the fluctuation dissipation theorem, that σ_I^2 should be proportional to χ_I. A reason for this discrepancy lies in the high level of intrinsic fluctuations in our system that makes this transition nonclassical. Instabilities or bifurcations occurring on highly fluctuating systems are commonly found in natural systems, and the literature reports transitions and symmetry breaking at high Re (see, e.g., Refs. [5–11,17,19–21]), but the corresponding theoretical tools are still not well settled. Existing studies of phase transitions in the presence of fluctuations generally consider systems in which an external noise—additive or multiplicative—is introduced [22]. In particular, it has been shown in models that multiplicative noise can produce an ordered symmetry-breaking state through a nonequilibrium phase transition [23]. This behavior could be at the origin of our observed transition. We can notice that, as Re increases, the turbulent momentization I_0 first increases and then decreases, contrary to the magnetization in the usual paraferromagnetic transition. This result is reminiscent of a reentrant noise-induced phase transition similar to that observed in the annealed Ising model [24,25]. The study of the evolution of I_0 and/or I_* with Re requires more statistics and is left for future work. Finally, our turbulent system, in which we can have access to both the spatiotemporal evolution of the states and the mean thermodynamic variables, appears as a unique tool to study out-of-equilibrium phase transitions in strongly fluctuating systems.

We thank K. Mallick for fruitful discussions. P.-P. C. was supported by Triangle de la Physique.

[1] L. D. Landau and E. M. Lifshitz, *Statisticheskaya Fisika* (Nauka, Moscow, 1976).
[2] P. Manneville, *Dissipative Structures and Weak Turbulence* (Academic, Boston, 1990).
[3] U. Frisch, *Turbulence—The Legacy of A. N. Kolmogorov* (Cambridge University Press, Cambridge, England, 1995).
[4] B. Hof, J. Westerweel, T. Schneider, and B. Eckhardt, Nature (London) **443**, 59 (2006).
[5] P. Tabeling *et al.*, Phys. Rev. E **53**, 1613 (1996).
[6] P. Tabeling and H. Willaime, Phys. Rev. E **65**, 066301 (2002).
[7] F. Ravelet, L. Marié, A. Chiffaudel, and F. Daviaud, Phys. Rev. Lett. **93**, 164501 (2004).
[8] F. Chillá, M. Rastello, S. Chaumat, and B. Castaing, Eur. Phys. J. B **40**, 223 (2004).
[9] N. Mujica and D. P. Lathrop, J. Fluid Mech. **551**, 49 (2006).
[10] F. Ravelet, A. Chiffaudel, and F. Daviaud, J. Fluid Mech. **601**, 339 (2008).
[11] R. Stevens *et al.*, Phys. Rev. Lett. **103**, 024503 (2009).
[12] C. Nore, L. S. Tuckerman, O. Daube, and S. Xin, J. Fluid Mech. **477**, 1 (2003).
[13] P. Chossat, Nonlinearity **6**, 723 (1993).
[14] J. Porter and E. Knobloch, Physica (Amsterdam) **201D**, 318 (2005).
[15] P.-P. Cortet *et al.*, Phys. Fluids **21**, 025104 (2009).
[16] Practically, $I(t)$ is computed from PIV data restricted to a meridian plane only, but, since azimuthal flow fluctuations are strong, time average over several rotation periods—statistically equivalent to spatial azimuthal averaging—estimates correctly the 3D value of $I(t)$ (see details in Ref. [15]).
[17] A. de la Torre and J. Burguete, Phys. Rev. Lett. **99**, 054101 (2007); J. Burguete and A. de la Torre, Int. J. Bifurcation Chaos Appl. Sci. Eng. **19**, 2695 (2009).
[18] B. Castaing, J. Phys. II (France) **6**, 105 (1996).
[19] M. Gibert *et al.*, Phys. Fluids **21**, 035109 (2009).
[20] R. Monchaux *et al.*, Phys. Rev. Lett. **98**, 044502 (2007).
[21] R. Monchaux *et al.*, Phys. Fluids **21**, 035108 (2009).
[22] N. G. van Kampen, *Stochastic Processes in Physics and Chemistry* (North-Holland, Amsterdam, 1981).
[23] C. Van den Broeck, J. M. R. Parrondo, and R. Toral, Phys. Rev. Lett. **73**, 3395 (1994).
[24] M. Thorpe and D. Beeman, Phys. Rev. B **14**, 188 (1976).
[25] W. Genovese, M. A. Munoz, and P. L. Garrido, Phys. Rev. E **58**, 6828 (1998).